IRSTI 29.19.16 https://doi.org/10.26577/phst20251229

Computer simulation of planar bifacial TOPCon solar cells by using Quokka 3 software

I.V. Zhirkov , A.M. Suleimenova ,
A.T. Sultanov* and N.B. Beisenkhanov

Kazakh-British Technical University, Almaty, Kazakhstan
*e-mail: a.sultanov@kbtu.kz

(Received May 8, 2025; received in revised form November 12, 2025; accepted November 26, 2025)

This study presents a comprehensive simulation-based analysis of bifacial Tunnel Oxide Passivated Contact (TOPCon) solar cells using the Quokka 3 software. It investigates the impact of different antireflection coatings and rear albedo variations on device performance. One of the main findings is the significant improvement in optical and electrical properties after applying MgF_2 antireflection coating on top of the cell. Structures with the addition of MgF_2 achieved low, uniform reflectance and increased light absorption across the full solar spectrum. Compared to structures without MgF_2, those with the coating exhibited superior external quantum efficiency (EQE) and reduced reflected photocurrent density (J_R) with the value of 3.38 mA/cm^2. Additionally, simulations revealed that increasing rear albedo values improved short-circuit current density (J_{sc}) and power conversion efficiency (PCE). The highest PCE of 27.37% and J_{sc} of 45.07 mA/cm^2 was obtained from a structure combining MgF_2 and a rear albedo of 0.3 Voc in this case was equal to 0.74V. These results confirm that optimizing both antireflection coatings and rear-side illumination can significantly improve the efficiency of bifacial TOPCon solar cells, offering a viable pathway for enhanced photovoltaic (PV) performance.

Keywords: Si solar cell, TOPCon solar cell, bifacial solar cell, Quokka 3, antireflection coatings.
PACS number(s): 84.60.Jt, 68.65.Ac, 42.70.−a.

1. Introduction

Since the development of silicon (Si)-based solar cells, the photovoltaic industry has undergone rapid growth. Fueled by the increasing global demand for clean and renewable energy, extensive research has been directed toward advancing solar cell technologies. This effort has led to numerous scientific achievements, including the recent emergence of Tunnel Oxide Passivated Contact (TOPCon) Si solar cells. Renowned for their excellent passivation properties, reduced recombination losses, and high-power conversion efficiency (PCE), TOPCon technology represents a promising advancement in the field.

The TOPCon solar cell was first developed by the Fraunhofer Institute for Solar Energy (ISE) Systems in Germany in 2013, showing an efficiency of 23.7%[1]. After several advancements such as optimizing the wafer resistivity and process flow, PCE was further elevated to higher values of ~25.7% and a high fill factor (FF) of ~83.3% in 2017 also at Fraunhofer ISE [2].

The main feature of fabricating TOPCon cells involves inserting a very thin interfacial silicon oxide (SiO_x) layer, typically around 1-2 nm, between doped polycrystalline Si (poly-Si) and crystalline Si (c-Si) layers, enhancing the collection of photogenerated carriers. Several research teams[1–5] have shown that combining a highly doped poly-Si layer with an ultrathin SiO_x layer provides low saturation current density (J_0<5 fA/cm²) and low contact resistivity (ρ_c<1 mΩ·cm²) simultaneously. This results in outstanding surface passivation with minimal recombination losses. The exceptional properties of the TOPCon structure are largely attributed to its key advantage: the c-Si wafer does not come into direct contact with the metal electrodes. This design helps reduce the Fermi level pinning (FLP) effect, thereby improving device performance and stability [3].

Recent developments in TOPCon structures have increased their market share and accelerated large-scale industrial production, supported by improved architecture such as integration with existing PERC lines and compatibility with high-efficiency silicon

tandem cells. Moreover, the configuration of bifacial TOPCon devices, generating energy from both the front and rear sides of the cell, has been actively explored in recent studies [6–9]. The front side functions like a standard solar cell, directly absorbing sunlight and converting it into electricity, while the rear side is designed to absorb light that is reflected off the ground or nearby surfaces, as well as diffused light from the atmosphere. This reflected and diffused solar radiation is measured by the term, called "albedo".

Albedo is the most significant factor for bifacial solar cells as it influences energy production. Surfaces with higher albedo reflect more light, consequently increasing the energy yield. Thus, optimizing the design of bifacial TOPCon cell can further improve energy output and become particularly attractive for large-scale solar power plants. Table 1 presents albedo values for different surfaces.

While experimental characterization of bifacial TOPCon cells requires significant efforts, computer simulations provide versatile and simple way to study this structure. In this context, Quokka 3, a finite-volume-based simulation software, allows full-cell modeling, becoming a valuable tool for analyzing the performance of solar cells [11, 12].

Table 1 – Albedo values for various types of surfaces [10].

Surface	Corrugated roof	Colored paint	Trees	Asphalt	Concrete	Grass	Ice
Albedo	0.1 – 0.15	0.15 – 0.35	0.15 – 0.18	0.05 – 0.2	0.25 – 0.3	0.25 – 0.3	0.3 – 0.5

Surface	Red/Brown roof tiles	Brick/Stone	Oceans	Old snow	White paint	Fresh Snow
Albedo	0.1 – 0.35	0.2 – 0.4	0.05 – 0.1	0.65 – 0.81	0.5 – 0.9	0.81 – 0.88

Computer simulations play a crucial role across all fields of scientific research, providing deeper insights and enabling more accurate predictions of experimental outcomes [13, 14]. In this research, we focus on a computer simulation of a bifacial TOPCon solar cell using Quokka 3 software. Our analysis includes utilization of antireflection coatings (ARC) based on transparent conductive oxides (TCO) such as Indium tin oxide (ITO), aluminum doped zinc oxide (AZO) and ARC based on magnesium fluoride (MgF_2) [15, 16]. Furthermore, we evaluated key performance metrics such as current-voltage (*J-V*) characteristics, reflectance spectra, external quantum efficiency (EQE), photocurrent density measurements and albedo-dependent characteristics of TOPCon solar cells with different ARCs. By comparing structures with different ARC of TOPCon solar cell, this study aims to identify the most efficient design. The findings contribute to a deeper understanding of bifacial TOPCon behavior and offer guidance for future development. By simulating bifacial solar cells, the study aims to highlight the performance advantages of bifacial operation and the influence of rear-side illumination in realistic operating environments.

2. Simulation details

Quokka 3 simulations were employed to demonstrate the performance differences between bifacial and standard TOPCon solar cells. Figure 1 illustrates the simulated geometries of both the bifacial and standard cells within the Quokka 3 software environment. The simulation parameters, which provides a detailed overview of the values used throughout the modeling process are summarized in Table 2. Throughout the study parameters such as ARC layer, rear albedo, and bifacial or standard structure mode were varied. Fixed parameters included bulk wafer properties (200 μm, 1 Ω·cm), poly-Si thickness (30 nm), doping densities, and recombination velocities, which were held constant based on typical literature values. For the bifacial cell simulations, the TOPCon+TCO structures were modeled by incorporating sheet resistance and saturation current density characteristics specific to bifacial designs. In contrast, the standard TOPCon solar cell was simulated using built-in Quokka 3 TOPCon structures for the rear side. This approach allowed for a clear comparison between the two architectures under consistent simulation conditions.

In the TOPCon solar cell structure, both the front and rear sides include poly-Si layers alongside a SiO_x tunneling layer. The poly-Si layer thickness was optimized to 30 nm, as this value was found to balance passivation quality and carrier transport efficiency [6, 17–19]. For the regular structure the rear side of the TOPCon solar cell was covered by silver (Ag) back electrode. A triple-layer coating composed of ITO-AZO-ITO was used as the transparent electrode on the front side. For the bifacial TOPCon solar cell ITO-AZO-ITO transparent electrode was used on both sides of the solar cell. To maximize optical performance of the TOPCon solar cell MgF_2 was used as an ARC on the top of the ITO-AZO-ITO transparent electrode. Figure 2 illustrates different structural combinations of TOPCon solar cells used in this work.

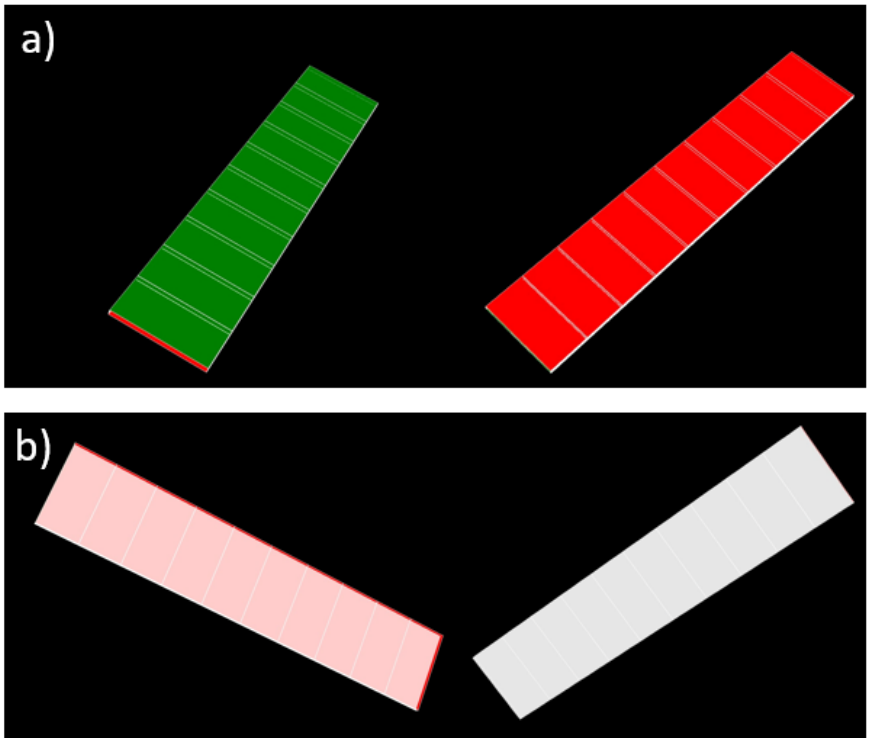

Figure 1 – 3D view of TOPCon solar cell derived from Quokka 3 software program : a) bifacial structure, b) standard structure.

Table 2 – Simulation parameters obtained from Quokka 3: Bulk parameters, external circuit, front n-type TOPCon + TCO layer, rear p-type TOPCon (Standard), rear p-type TOPCon (Bifacial) + TCO parameters.

Bulk parameters	
Dimensions	2
Thickness	200 µm
Width	18000 µm
Resistivity(Bulk)	1 Ohm*cm
Facing angle front/rear	0
Doping type	p-type
Fundamental electron surface recombination velocity(n)	100 cm/s
Fundamental electron surface recombination velocity(p)	100 cm/s
Defect energy relative to intrinsic energy	0 eV
Ilumination spectrum Rear/Front	AM1.5g

Continuation of the table

Ilumination scale Frontside	1
Ilumination scale Rearside	(0,0.3) with step 0.02
External cicuit	
Rseries	0.46 Ohmcm^2
Rshunt	3.5E3 Ohmcm^2
Saturation current density of external diode	0 Acm^{-2}
Ideality factor of external diode	2
front n-type TOPCon +TCO layer	
ConductionType	n-type
Rsheet	90.58 Ohm/square
Non Contacted Recombination *Jo*	2 fA/cm^2
Contacted Recombination	20 fA/cm^2
Thickness(poly-Si)	30nm
DopingDensity	1E20 cm^{-3}
Contact shape	Rectangle
Contact size	30 µm
Contact pitch	1800 µm
Contact repetition	11
Contact Ohmic Resistivity	5E-5 Ohmcm^2
Metal Rsheet	0.003 Ohm
rear p-type TOPCon (standard)	
Conduction type	p-type
DopingDensity	1E19 cm^{-3}
Thickness	30 nm
fundamental electron surface recombination velocity	10 cm/s
fundamental hole surface recombination velocity	10 cm/s
Contact shape	Full
Contact size	18000 µm
Contact Ohmic Resistivity	5E-5 Ohmcm^2
Metal Rsheet	0.003 Ohm
rear p-type TOPCon (Bifacial) +TCO	
Conduction type	p-type
Rsheet	90.58 Ohm/square
NonContactedRecombination *Jo*	2 fA/cm^2
ContactedRecombination	20 fA/cm^2
Thickness(poly-Si)	30nm
DopingDensity	1E20 cm^{-3}
Contact shape	Rectangle
Contact size	30 µm
Contact pitch	1800 µm
Contact repetition	11
Contact Ohmic Resistivity	5E-5 Ohmcm^2
Metal Rsheet	0.003 Ohm

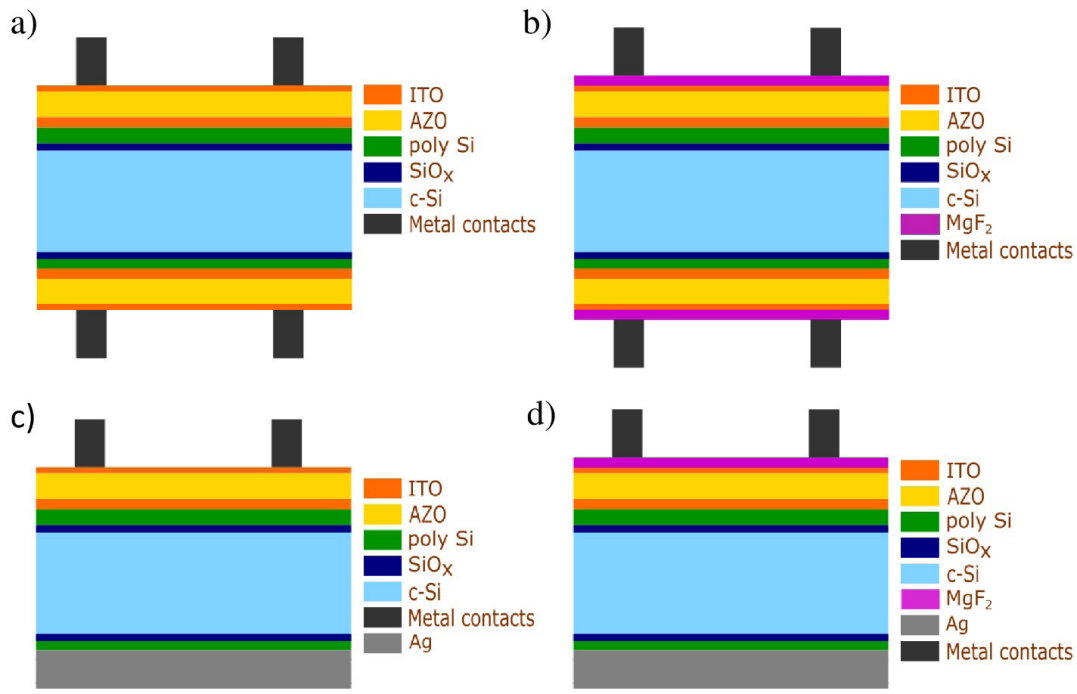

Figure 2 – Two-dimensional schematics of c-Si-based TOPCon solar cell:
a) Simplified cell structure without MgF_2 and Ag, b) Cell structure with MgF_2 on both sides without Ag layer,
c) Simplified cell structure with Ag at the bottom d) Cell structure with MgF_2 on top and Ag at the bottom.

OPAL 2 optical simulator [20] was used to optimize the thickness of the transparent TCO electrode and MgF_2 ARC for improved optical performance. During optimizations the goal was set to achieve maximum photon current absorbed in the active layer. Due to the layer number limitations of the OPAL 2 simulator, the thicknesses of the ITO-AZO-ITO multilayer were initially optimized as a standalone structure. Once the optimal configuration was determined, the MgF_2 layer was optimized separately. To accommodate the simulator's constraints, the previously optimized ITO-AZO-ITO structure was modeled as a single ITO-equivalent layer, with the MgF_2 layer added on top of this simplified model.

To further analyze the optical properties of the considered TOPCon solar cells, reflectance, parasitic absorption, and absorption within the active area were simulated using SCOUT software [21]. The absorption characteristics of each layer were evaluated individually, and the total parasitic absorption was calculated as the sum of absorption in all layers except the substrate.

The optical constants (n and k) for ITO and AZO were taken from the works of [22, 23]. The optical constants for MgF_2 are taken from [24], as linked in the OPAL 2 database. All other layers, including the substrate and back layers, were obtained from the SCOUT software [21].

3. Results and discussion

For accurate modeling and simulation of the optical behavior of the TOPCon solar cell, reliable refractive index (n) and extinction coefficient (k) data are essential. Figure 3 shows the wavelength-dependent optical constants for different materials used in the TOPCon solar cell. AZO exhibits a lower extinction coefficient than ITO, which ensures higher transmittance of ITO-AZO-ITO structure compared to an ITO-only structure. The ITO-AZO-ITO structures were examined in detail in our previous work[25].

Across the entire range, MgF_2 shows minimal extinction coefficient values, highlighting its highly transparent dielectric property. Moreover, it is well established that to minimize reflectance from a solar cell surface, it is essential to use materials with a gradually increasing refractive index from air to the substrate. The optimal refractive index n for the material used as an ARC can be calculated using the formula [26]:

$$r = \left[\frac{n_{air}\, n_s - n^2}{n_{air}\, n_s + n^2}\right]^2, \qquad (1)$$

where n_s is a refractive index of the substrate, n_{air} is a refractive index of air and n is a refractive index of the film.

According to the calculations refractive index of MgF_2 (~1.38) is suitable to reduce reflection from TOPCon solar cell. Thus, in this work, TOPCon solar cell are considered with and without MgF_2 ARC.

Figure 4a shows the simulated reflectance spectra of the TOPCon structures with and without the MgF_2 ARC over the 300–1200 nm wavelength range. For reference, the solar irradiation spectrum is shown in the background. The structure with MgF_2 layer shows relatively low and constant reflectance throughout the spectrum, suggesting effective antireflection behavior. Moreover, it experiences a noticeable decrease in reflectance between 600–700 nm. This reduction in reflectance is attributed to the low refractive index of MgF_2, which reduces the refractive index mismatch between the underlying layers and air. The refractive index of MgF_2 exhibits only minor variation across the entire solar spectrum while other refractive indexes experiencing constant decrease on the most part of spectrum, with the wavelength range of 600–700 nm providing the most noticeable smooth refractive index gradient between the underlying layers and air. However, the structure without MgF_2 demonstrates a sharp reduction of reflectance at around 600 nm, suggesting that careful design of multilayer structure can achieve low reflectance at specific wavelengths. Overall, while the addition of MgF_2 layer provides more consistent antireflective behavior across the broad spectrum, the structure without MgF_2 offers potential for targeted wavelength optimization through multilayer structure engineering.

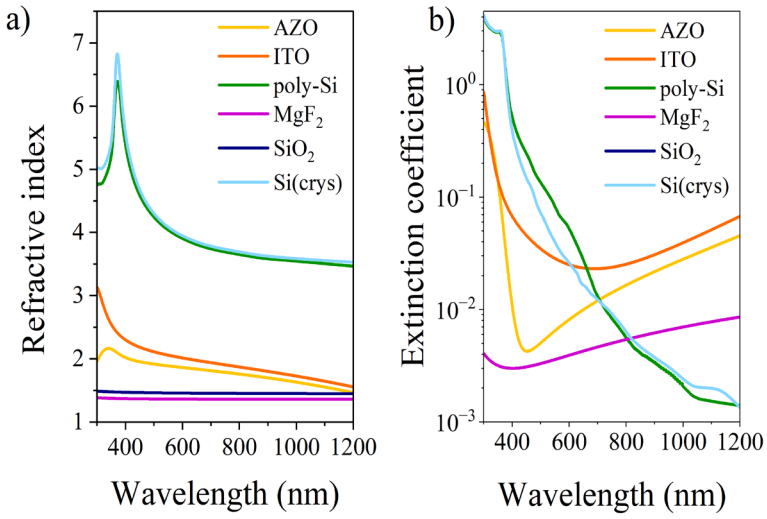

Figure 3 – Optical properties: a) Refractive index and b) extinction coefficient as functions of wavelength for various materials (AZO, ITO, poly-Si, MgF_2, SiO_2, Si).

Figure 4b illustrates the EQE simulations for structures with and without MgF_2, which is significantly influenced by the optical constants n and k, where the refractive index n determines the proportion of photons reflected at the interfaces between layers, while the extinction coefficient k governs the extent to which photons can penetrate into the bulk layer and the fraction that is transmitted without being absorbed. The structure with MgF_2 layer exhibits higher performance across most of the wavelength range compared to the structure without MgF_2. This is also evident in the calculated current density (J), which shows that the final J value for the solar cell with MgF_2 ARC is higher. However, due to the decrease in reflectance between 450 nm and 700 nm, the structure without MgF_2 shows slightly better performance in this region. Overall, the addition of the MgF_2 layer improves the EQE, indicating enhanced light management and reduced reflection due to the antireflective effect provided by MgF_2.

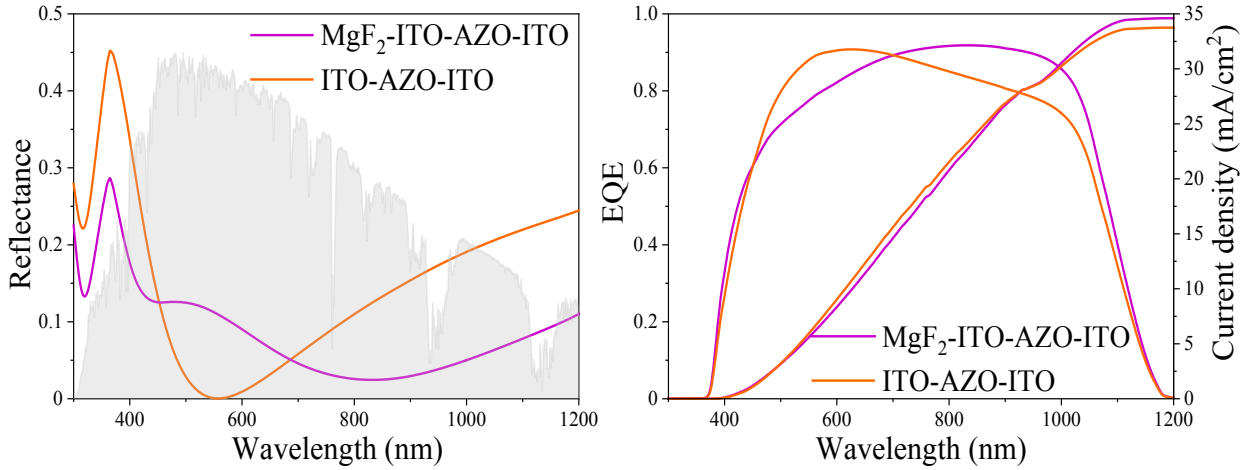

Figure 4 – a) Reflectance spectra of ITO-AZO-ITO and MgF_2-ITO-AZO-ITO structures; b) EQE measurements for standard TOPCon solar cell with ITO-AZO-ITO and MgF_2-ITO-AZO-ITO ARC.

To provide a comprehensive description of the optical properties of the structure, photon current density calculations were performed. 3 main characteristics were calculated: reflected photon current density (J_R), parasitic absorption current density (J_{PA}) and absorbed photon current density in the substrate (J_{Abulk}). As optimizing useful absorption is essential for solar cell performance, the $J_{R,}$ J_{PA} and J_{Abulk} was determined for the wavelength intervals of 300–1200 nm by the following equation [27]:

$$J_x = \int_{\lambda 2}^{\lambda 1} X(\lambda) F(\lambda) q d\lambda, \quad (2)$$

where X (λ) is reflectance, parasitic absorption or absorption in the bulk, F (λ) is the incident photon flux density of AM1.5G irradiation, q is the elementary charge, and λ is the wavelength.

Figure 5 provides J_R, J_{PA}, J_{Abulk} calculations for different structures. Comparing bifacial and standard structures. According to the result all current density values show minimal differences, indicating that the back reflection from the rear Ag electrode is negligible. However, the addition of the MgF_2 layer to the ITO-AZO-ITO structure leads to significant decline of J_R from 5.44 to 3.38 mA/cm², subsequently refining J_{PA} and J_{Abulk} values This suggests that addition of MgF_2 acts effectively, redirecting previously reflected light into the active layer and enhancing useful absorption.

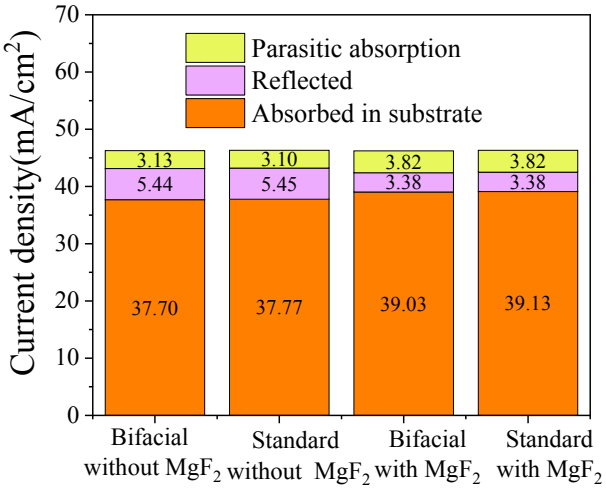

Figure 5 – Photo current density measurements for four configurations (Bifacial (ITO-AZO-ITO); Standard (ITO-AZO-ITO); Bifacial (MgF_2-ITO-AZO-ITO); Standard (MgF_2-ITO-AZO-ITO). Three types of current densities are compared: Reflected current (J_R), parasitic absorption current (J_{PA}), current absorbed in the substrate (J_{Abulk}).

Figure 6 presents the *J–V* characteristics of TOPCon solar cells with and without a MgF_2 ARC under varying rear-side albedo conditions. For clarity, Figures 6a and 6b depict the results for a standard and a bifacial TOPCon solar cell, with albedo intensities varying from 0 to 0.3 suns in 0.1 increments. Even in the absence of rear illumination (0 suns), the bifacial TOPCon solar cell exhibits a PCE of 20.56%, slight-

ly lower than that of the reference structure with a Ag back reflector (20.94%). This trend remains consistent for both MgF_2-coated and uncoated devices. Upon introducing a modest rear albedo of 0.1 suns, the bifacial structure demonstrates an almost 2% absolute increase in PCE, emphasizing the sensitivity of the device to even minor enhancements in rear-side illumination. This improvement is primarily attributed to the significant rise in short-circuit current density (J_{sc}), while the open-circuit voltage (V_{oc}) remains nearly constant across all albedo levels.

Figures 6c and 6d provide a more detailed analysis of the bifacial configuration, displaying the evolution of *J–V* parameters as the albedo varies from 0 to 0.3 suns in finer steps of 0.02. The results show an almost linear increase in J_{sc} with albedo, while V_{oc} changes slightly, from 0.73 to 0.74 V. These findings confirm that the observed PCE enhancement is predominantly governed by the increase in photocurrent. Furthermore, devices incorporating MgF_2 ARC consistently outperform those without it under all albedo conditions. The MgF_2 layer, in conjunction with enhanced rear illumination, improves light trapping and optical coupling, thereby boosting the internal photon generation rate. These outcomes highlight that increasing back albedo, especially when combined with optimized optical coatings, is a highly effective strategy for enhancing the photocurrent and overall performance of TOPCon solar cells.

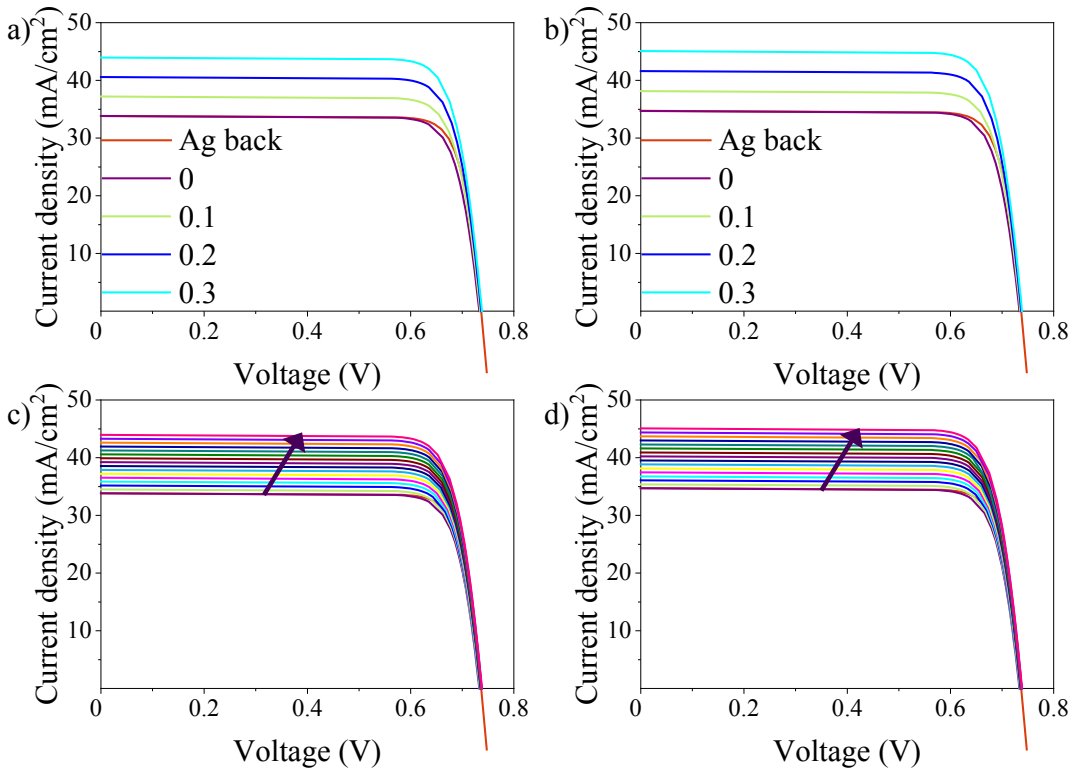

Figure 6 – *J–V* Characteristics Under Varying Back Albedo for structures with MgF_2 on the top and without MgF_2: a),b) shows changes to *J*-V curve of bifacial structure in comparison to standard Ag back solar cells, pictures c),d) shows changes to *J*-V curve with increase of back albedo from 0 to 0.3 with the step of 0.02(arrow show direction of increased albedo).

Tables 3 and 4 presents extensive data results based on Quokka 3 simulation. From previous discussion it was mentioned that J_{sc} increases with increase of back albedo and Tables 3 and 4 proves this for both cases with and without MgF_2. The same is true for PCE. For the structures without MgF_2, the highest value of PCE is achieved at 26.69 %, while TOPCon solar cell with MgF_2 ARC on top show the maximum value of 27.37 %. This results also shows precisely the point where V_{oc} for bifacial solar cell reaches the

value for standard TOPCon solar cell. For TOPCon solar cells without MgF_2 the required albedo is 0.12 suns while with MgF_2 implemented cells 0.08 suns albedo is already enough. Even though bifacial solar cell provides better result for PCE, V_{oc} and J_{sc} it's important to point out that standard solar cells for both cases showed maximum FF while bifacial structure showed decrease in FF with increase of albedo.

Table 3 – Bifacial TOPCon solar cell characteristics: open-circuit voltage (V_{oc}), short-circuit current density (J_{sc}), fill factor (FF), power conversion efficiency (PCE) values for structures without MgF_2.

Optical Rear Illumination Scale Without MgF_2	V_{oc} (V)	J_{sc} (mA/cm^2)	FF (%)	PCE (%)
Ag back	0.74	33.84	83.99	20.94
0	0.73	33.81	82.93	20.56
0.02	0.73	34.49	82.89	20.97
0.04	0.73	35.16	82.85	21.38
0.06	0.73	35.84	82.81	21.79
0.08	0.73	36.51	82.76	22.20
0.1	0.73	37.19	82.73	22.61
0.12	0.74	37.86	82.69	23.02
0.14	0.74	38.54	82.65	23.43
0.16	0.74	39.22	82.60	23.84
0.18	0.74	39.89	82.56	24.25
0.2	0.74	40.57	82.52	24.66
0.22	0.74	41.24	82.47	25.07
0.24	0.74	41.92	82.43	25.47
0.26	0.74	42.59	82.38	25.88
0.28	0.74	43.27	82.34	26.29
0.3	0.74	43.94	82.29	26.69

Table 4 – Bifacial TOPCon solar cell characteristics: open-circuit voltage (V_{oc}), short-circuit current density (J_{sc}), fill factor (FF), power conversion efficiency (PCE) values for structures with MgF_2.

Optical Rear Illumination Scale with MgF_2	V_{oc} (V)	J_{sc} (mA/cm^2)	FF (%)	PCE (%)
Ag back	0.74	34.71	83.94	21.48
0	0.73	34.68	82.88	21.08
0.02	0.73	35.37	82.84	21.51
0.04	0.73	36.06	82.79	21.93
0.06	0.73	36.76	82.75	22.35
0.08	0.74	37.45	82.71	22.77
0.1	0.74	38.14	82.67	23.19
0.12	0.74	38.83	82.63	23.61
0.14	0.74	39.53	82.58	24.03
0.16	0.74	40.22	82.54	24.45
0.18	0.74	40.91	82.49	24.87

Continuation of the table

Optical Rear Illumination Scale with MgF_2	V_{oc} (V)	J_{sc} (mA/cm^2)	FF (%)	PCE (%)
0.2	0.74	41.60	82.45	25.29
0.22	0.74	42.30	82.40	25.70
0.24	0.74	42.99	82.36	26.12
0.26	0.74	43.68	82.31	26.54
0.28	0.74	44.38	82.26	26.95
0.3	0.74	45.07	82.21	27.37

Overall, the findings underscore the significance of combining advanced ARC strategies–such as MgF_2-capped multi-layer designs–with effective utilization of bifacial architectures. The implementation of ARC structure allowed for better energy distribution between used and not used energy. While implementation of rear side illumination explicitly shows increase in J_{sc}. Such integrated optimization not only boosts the efficiency of TOPCon cells but also maximizes their energy yield in real-world operating conditions. The achieved efficiency of 27.37% under a rear albedo of 0.3 with MgF_2 outperforms many reported TOPCon structures in the literature, which typically range between 23–26% [2, 6–8]. Consequently, compared to existing TOPCon approaches, the practical difference of the model lies in integration of MgF_2/ITO/AZO/ITO ARCs and rear albedo effects with a bifacial operation, allowing for simultaneous enhancement of optical and electrical performance. This research reinforces the potential of MgF_2-enhanced bifacial TOPCon solar cells as a viable and efficient solution for next-generation photovoltaic technologies.

It is important to note, however, that our simulations have some limitations. The optical modeling in OPAL 2 considered only the front-side texture and assumed an idealized Lambertian rear reflector, while SCOUT assumed planar, continuous layers. Electrically, Quokka 3 operates in 2D and does not capture all 3D carrier transport effects. Furthermore, all simulations assumed ideal interfaces and material properties; real-world fabrication imperfections may lead to slightly lower performance. Experimental verification of the simulated structures is therefore needed, including MgF_2-coated bifacial TOPCon cells, to confirm the simulation result

4. Conclusions

In conclusion, this study presents a comprehensive simulation-based investigation of bifacial TOPCon solar cells, with modeling conducted using Quokka 3 software. The structural design and optical characteristics of these cells were thoroughly examined with the aid of OPAL 2 and SCOUT softwares, enabling precise analysis of light behavior and internal device parameters. A key focus was placed on evaluating various ARC configurations, specifically triple-layered ITO-AZO-ITO structures, both with and without the inclusion of an MgF_2 top layer. It was found that the refractive index of MgF_2 is suitable for reducing reflection from TOPCon solar cells with ITO/AZO/ITO transparent electrode. The optical modeling revealed that the integration of an MgF_2 layer on top of the ARC significantly enhances the optical response of the solar cell by achieving lower and more uniform reflectance across the spectrum under investigation with a noticeable decrease between 600-700 nm. This improvement in light management leads to better photon absorption, ultimately translating into enhanced electrical performance. The optimized structure demonstrated a measurable gain in EQE. Furthermore, the addition of MgF_2 effectively redirects previously reflected light into the active layer, enhancing useful absorption. As a result, a significant decline in J_R from 5.44 to 3.38 mA/cm² was observed, leading to improved J_{PA} and J_{Abulk} values. Further analysis focused on the impact of rear-side illumination, modeled through varying rear albedo conditions. Back reflection from the rear Ag electrode was found to be negligible. It has been established that at 0 suns albedo, PCE of bifacial solar cells was only slightly lower than of solar cells

with Ag back (20.56 to 20.94% respectively) and this trend was similar for both structures with and without MgF_2 ARC. Results indicated that increasing the albedo positively influences key electrical parameters of the *J-V* curve, notably the J_{sc} and PCE with V_{oc} slightly changing from 0.73 to 0.74. The highest efficiency, recorded at 27.37%, was achieved under a rear albedo of 0.3 when the cell incorporated the MgF_2-enhanced ARC structure. This highlights the critical role of rear-side reflectivity in bifacial solar cell performance, emphasizing the importance of optimizing both front and rear interfaces. Additionally, the computer simulation highlights the need for future experimental validation of the proposed structures, given their outstanding simulated performance.

Acknowledgements. The research was funded by the Science Committee of the Ministry of Science and Higher Education of the Republic of Kazakhstan (Grant No. AP19680267).

References

1. Rohatgi A., Rounsaville B., Ok Y. W., Tam A. M., Zimbardi F., Upadhyaya A. D., Tao Y., Madani K., Richter A., Benick J., Hermle M. Fabrication and modeling of high-efficiency front junction n-type silicon solar cells with tunnel oxide passivating back contact // IEEE Journal of Photovoltaics. – 2017. – Vol. 7. – Pp. 1236–1243. https://doi.org/10.1109/JPHOTOV.2017.2715720

2. Feldmann F., Reichel C., Müller R., Hermle M. The application of poly-Si/SiOx contacts as passivated top/rear contacts in Si solar cells // Solar Energy Materials and Solar Cells. – 2017. – Vol. 159. – Pp. 265–271. https://doi.org/10.1016/j.solmat.2016.09.015

3. Ullah H., Czapp S., Szultka S., Tariq H., Qasim U. Bin, Imran H. Crystalline silicon (c-Si) based tunnel oxide passivated contact (TOPCon) solar cells: A review // Energies. – 2023. – Vol. 16. – Art. 715. https://doi.org/10.3390/en16020715

4. Römer U., Peibst R., Ohrdes T., Lim B., Krügener J., Wietler T., Brendel R. Ion implantation for poly-Si passivated back-junction back-contacted solar cells // IEEE Journal of Photovoltaics. – 2015. – Vol. 5. – Pp. 507–514. https://doi.org/10.1109/JPHOTOV.2014.2382975

5. Peibst R., Römer U., Larionova Y., Rienäcker M., Merkle A., Folchert N., Reiter S., Turcu M., Min B., Krügener J., Tetzlaff D., Bugiel E., Wietler T., Brendel R. Working principle of carrier selective poly-Si/c-Si junctions: Is tunnelling the whole story? // Solar Energy Materials and Solar Cells. – 2016. – Vol. 158. – Pp. 60–67. https://doi.org/10.1016/j.solmat.2016.05.045

6. Wang Q., Peng H., Gu S., Guo K., Wu W., Li B., Li L., Yuan N., Ding J. High-efficiency n-TOPCon bifacial solar cells with selective poly-Si based passivating contacts // Solar Energy Materials and Solar Cells. – 2023. – Vol. 259. – Art. 112458. https://doi.org/10.1016/j.solmat.2023.112458

7. Wu W., Jolywood J. B., Bao J., Ma L., Chen C., Liu R., Qiao Z., Chen J., Liu Z. Development of industrial n-type bifacial TOPCon solar cells and modules // 37th European Photovoltaic Solar Energy Conference and Exhibition. – 2019. – Pp. 100–102. https://doi.org/10.4229/EUPVSEC20192019-2BP.1.5

8. Chen Y., Chen D., Liu C., Wang Z., Zou Y., He Y., Wang Y., Yuan L., Gong J., Lin W., Zhang X., Yang Y., Shen H., Feng Z., Altermatt P. P., Verlinden P. J. Mass production of industrial tunnel oxide passivated contacts (i-TOPCon) silicon solar cells with average efficiency over 23% and modules over 345 W // Progress in Photovoltaics: Research and Applications. – 2019. – Vol. 27. – Pp. 827–834. https://doi.org/10.1002/pip.3180

9. Jain A., Choi W. J., Huang Y. Y., Klein B., Rohatgi A. Design, optimization, and in-depth understanding of front and rear junction screen-printed double-side passivated contacts solar cells // Conference Record of the IEEE Photovoltaic Specialists Conference. – 2020. – Pp. 1339–1343. https://doi.org/10.1109/PVSC45281.2020.9300805

10. Kotak B., Eng Y., Gul BEng M. S., Muneer T., Ivanova S. Investigating the impact of ground albedo on the performance of PV systems // CIBSE Technical Symposium, London, UK, April 16-17, 2015. https://researchportal.hw.ac.uk/en/publications/investigating-the-impact-of-ground-albedo-on-the-performance-of-p/ (available on December 17, 2025).

11. Fell A., Altermatt P. P. A detailed full-cell model of a 2018 commercial PERC solar cell in Quokka3 // IEEE Journal of Photovoltaics. – 2018. – Vol. 8. – P. 1443–1448. https://doi.org/10.1109/JPHOTOV.2018.2863548

12. Kowsar A., Debnath S. C., Shafayet-Ul-Islam Md., Hossain M. J., Hossain M., Chowdhury A. K., Hashmi G., Farhad S. F. U. An overview of solar cell simulation tools // Solar Energy Advances. – 2025. – Vol. 5. – Art. 100077. https://doi.org/10.1016/j.seja.2024.100077

13. Solodovnik A., Kleksin R., Leontyev P., Useinov B., Markova A., Kassimova S. Revealing the noctilucent cloud fields structure by software processing of satellite images // Physical Sciences and Technology. – 2025. – Vol. 12. – Pp. 4–13. https://doi.org/10.26577/phst20251211

14. Vorobyova O., Sokolov D., Korshikov Y. Modeling of thermal distribution on cryosurface for low temperatures // Physical Sciences and Technology. – 2025. – Vol. 12. – No. 1–2. – Pp. 115–120. https://doi.org/10.26577/phst202512111

15. Kemelbekova A., Lebedev I. A., Grushevskaya E. A., Murzalinov D. O., Fedosimova A. I., Kemelbekova A. E., Kazhiev Zh. Sh., Zhaysanbayev Zh. K., Temiraliyev A. T. The effect of deposition technique on formation of transparent conductive coatings of SnO_2 // Physical Sciences and Technology. – 2022. – Vol. 9. – Pp. 37–44. https://doi.org/10.26577/phst.2022.v9.i1.05

16. Chavan G. T., Kim Y., Khokhar M. Q., Hussain S. Q., Cho E.-C., Yi J., Ahmad Z., Rosaiah P., Jeon C.-W. A brief review of transparent conducting oxides (TCO): the influence of different deposition techniques on the efficiency of solar cells // Nanomaterials. – 2023. – Vol. 13. – No. 7. – Art. 1226. https://doi.org/10.3390/nano13071226

17. Grübel B., Nagel H., Steinhauser B., Feldmann F., Kluska S., Hermle M. Influence of plasma-enhanced chemical vapor deposition poly-Si layer thickness on the wrap-around and the quantum efficiency of bifacial n-TOPCon solar cells // Physica Status Solidi (A) Applications and Materials Science. – 2021. – Vol. 218. – Art. 2100156. https://doi.org/10.1002/pssa.202100156

18. Yan X., Suhaimi F. Bin, Xu M., Yang J., Zhang X., Wang Q., Jin H., Shanmugam V., Duttagupta S. Development of ultra-thin doped poly-Si via LPCVD and ex-situ tube diffusion for passivated contact solar cell applications // Solar Energy Materials and Solar Cells. – 2020. – Vol. 209. – Art. 110458. https://doi.org/10.1016/j.solmat.2020.110458

19. Ditsougou J., Desrues T., Kaminski A., Dubois S. Optimization of poly-Si/SiOx passivated contacts for crystalline silicon bottom cells applications // SiliconPV Conference Proceedings. – 2025. – Vol. 2. https://doi.org/10.52825/siliconpv.v2i.1310

20. McIntosh K. R., Baker-Finch S. C. OPAL 2: Rapid optical simulation of silicon solar cells // 38th IEEE Photovoltaic Specialists Conference. – 2012. – Pp. 000265–000271. https://doi.org/10.1109/PVSC.2012.6317616

21. Theiss W. Hard- and software for optical spectroscopy. – Available at: https://www.wtheiss.com/ (available on December 15, 2025).

22. Nussupov K. K., Beisenkhanov N. B., Kusainova A. Z., Shynybayev D. S., Zhirkov I. V., Sultanov A. T. Influence of the RF magnetron sputtering power on the optical and electrical properties of AZO films // Physical Sciences and Technology. – 2023. – Vol. 10. – No. 2. – Pp. 28–32. https://doi.org/10.26577/phst.2023.v10.i2.03

23. Rakhimova A. Zh., Zhirkov I. V., Nussupov K. Kh., Beisenkhanov N. B., Sultanov A. T. Effect of oxygen flow on electrical and optical properties of ITO films synthesized by magnetron sputtering method // Herald of the Kazakh-British Technical University. – 2023. – Vol. 20. – P. 109–117. https://doi.org/10.55452/1998-6688-2023-20-4-109-117

24. Siqueiros J. M., Machorro R., Regalado L. E. Determination of the optical constants of MgF_2 and ZnS from spectrophotometric measurements and the classical oscillator method // Applied Optics. – 1988. – Vol. 27. – Pp. 2549–2553. https://doi.org/10.1364/AO.27.002549

25. Sultanov A., Zhirkov I., Nussupov K., Kusainova A., Abdyldayeva N., Beisenkhanov N. Investigation on optical and electrical properties of multilayer ITO/AZO/ITO transparent conductive oxides // Optical Materials. – 2024. – Vol. 155. – Art. 115850. https://doi.org/10.1016/j.optmat.2024.115850

26. Raut H. K., Ganesh V. A., Nair A. S., Ramakrishna S. Anti-reflective coatings: A critical, in-depth review // Energy and Environmental Science. – 2011. – Vol. 4. – Pp. 3779–3804. https://doi.org/10.1039/C1EE01297E

27. Sultanov A., Mussakhanuly N., Kusainova A., Parkhomenko H. P., Yerlanuly Y., Nussupov K., Ng A., Beisenkhanov N., Jumabekov A. N. Utilizing MoOx-Au-MoOx trilayers as transparent top electrodes in 2-terminal monolithic Si/perovskite tandem solar cells // Applied Physics A: Materials Science and Processing. – 2025. – Vol. 131. – Pp. 1–10. https://doi.org/10.1007/s00339-025-08425-x

Information about authors:

Zhirkov Ilya – Junior Researcher at the "Laboratory of Alternative Energy and Nanotechnology", Master Student at the Kazakh-British Technical University (Almaty, Kazakhstan, e-mail: il_zhirkov@kbtu.kz).

Suleimenova Aiganym – Lab Assistant at the "Laboratory of Alternative Energy and Nanotechnology", Bachelor student at the Kazakh-British Technical University (Almaty, Kazakhstan, e-mail: aiga_suleimenova@kbtu.kz).

Sultanov Asanali – PhD student at the Kazakh-British Technical University, Head of "Laboratory of Alternative Energy and Nanotechnology" at the Kazakh-British Technical University (Almaty, Kazakhstan, e-mail: a.sultanov@kbtu.kz).

Beisenkhanov Nurzhan – Doctor of Physical and Mathematical Sciences, Professor, Member of AAAS and ACS, Chief Researcher, Dean of SMS&GT at the Kazakh-British Technical University (Almaty, Kazakhstan, e-mail: n.beisenkhanov@kbtu.kz).